## Electrical bistability of skeletal muscle membrane

Geukes Foppen, R.J.

**Publication date**
2005

R. J. Geukes Foppen · J. Siegenbeek van Heukelom

# Isoprenaline-stimulated differential adrenergic response of $K^+$ channels in skeletal muscle under hypokalaemic conditions

Received: 28 October 2002 / Revised: 3 February 2003 / Accepted: 11 February 2003 / Published online: 15 March 2003


**Abstract** The mechanism underlying the hyperpolarization induced by isoprenaline in mouse lumbrical muscle fibres was studied using cell-attached patch and intracellular membrane potential ($V_m$) recordings. Sarcolemmal inwardly rectifying $K^+$ channels ($K_{IR}$: 45 pS) and $Ca^{2+}$-activated $K^+$ channels (BK: 181 pS) were identified. Exposure to isoprenaline closed $K_{IR}$ channels and increased BK channel activity. This increase was observed as a shift from 50 to –40 mV in the voltage dependence of channel activation. Isoprenaline prevented hysteresis of $V_m$ when the extracellular $[K^+]$ fell below 3.8 mM. This hysteresis was due to the properties of the $K_{IR}$. The effects of chloride transport and isoprenaline on $V_m$ did not interact purely competitively, but isoprenaline could prevent the depolarization induced by hyperosmotic media equally as well as bumetanide, which inhibits the $Na^+/K^+/2Cl^-$ cotransporter. In lumbrical muscle this leads to hyperpolarization, but this might vary among muscles. The switch from $K_{IR}$ to BK as the component of total $K^+$ conductance was due to isoprenaline.

**Keywords** Isoprenaline · Membrane potential · $\beta_2$-Adrenoceptor · Skeletal muscle · Inwardly rectifying potassium channels · $Ca^{2+}$-activated potassium channels · Hypokalaemic periodic paralysis · $Na^+/K^+/2Cl^-$ cotransporter

## Introduction

In skeletal muscle catecholamines are important for cellular $K^+$ homeostasis, for the membrane potential ($V_m$) [32, 33, 37] and for potentiating force development [3]. In studies of the electrical effects of $\beta_2$-adrenergic stimulation of skeletal muscle cells, invariably membrane hyperpolarization has been observed. In mouse lumbrical [37] and diaphragm muscle fibres [41] this effect is related mainly to an increase in $K^+$ permeability ($P_K$), and in the rat diaphragm muscle the permeability ratio $P_{Na}:P_K$ falls [20]. The first indication that in skeletal muscle the isoprenaline-activated $P_K$ behaves differently from the commonly present inwardly rectifying $K^+$ channel ($K_{IR}$) is that inhibition of this activated $P_K$ requires a higher $[Ba^{2+}]_o$ than that needed to block $K_{IR}$ [37]. This differential sensitivity suggests the involvement of different types of $K^+$ conductances. $Ba^{2+}$ blocks many $K^+$ channels at different concentrations: $K_{IR}$ channels [35], large-conductance, $Ca^{2+}$-activated channels (BK) [39] and delayed rectifier channels [1]. In parallel, $Ba^{2+}$ treatment is thought to elicit responses comparable to episodes of hypokalaemic periodic paralysis by affecting $K^+$ channel function in mammalian skeletal muscle [11]. Resting membrane potentials of many tissues are bistable (i.e. exhibit two different values of $V_m$ under identical experimental conditions; for references see [13]). This bistability is often related to the non-linear properties of $K_{IR}$.

The range of extracellular $[K^+]$ ($[K^+]_o$) over which bistability occurs is also dependent on cellular chloride transport [13]. This transport can be modulated by hypertonicity of the medium and can be inhibited by the $Na^+/K^+/2Cl^-$ cotransporter inhibitor bumetanide and by the chloride conductance inhibitor anthracene-9-carboxylic acid (9-AC). Both inhibitors cause membrane hyperpolarization [38]. An influence of protein phosphorylation on the $Na^+/K^+/2Cl^-$ cotransporter has also been demonstrated in ferret erythrocytes [9] and on the chloride conductance in rabbit ventricular myocytes [15]. Hence, the role of $Cl^-$ transport was also addressed in the present study, because it could be involved in the hyperpolarizing response induced by isoprenaline (Iso).

R. J. Geukes Foppen · J. Siegenbeek van Heukelom (✉)
Swammerdam Institute for Life Sciences,
University of Amsterdam,
Box 94084, 1098 GB Amsterdam, The Netherlands
e-mail: siegenbeek@science.uva.nl
Tel.: +31-20-5257642
Fax: +31-20-6738738

## Materials and methods

### Animals and choice of preparation

Female white Swiss mice were housed and used in accordance with Dutch regulations concerning animal welfare. Directly preceding the experiments, the mice, weighing 20–40 g, were killed by cervical dislocation. Two types of preparations from the lumbrical muscle were used. For patch clamping we used isolated cells and for intracellular microelectrodes we isolated a muscle bundle as described earlier [13]. Some intracellular microelectrode experiments were carried out in soleus muscle fibres that were dissected and handled similarly. It is evident that the differences in preparation, age, weight or experiment duration can lead to data scatter.

### Cell-attached patch-clamp experiments

Bundles from the lumbrical muscle were dissected from the hind limb in cold and freshly gassed (95% $O_2$/5% $CO_2$) modified Krebs-Henseleit solution (KH) containing (in mM): NaCl 117.5, KCl 5.7, $NaHCO_3$ 25.0, $NaH_2PO_4$ 1.2, $CaCl_2$ 2.5, $MgCl_2$ 1.2 and glucose 5.6, pH 7.35–7.45 (288 mOsm). Subsequently, the bundles were transferred to a KH solution containing 3 mg/ml collagenase (type 1). The enzymatic dissociation proceeded for 90 min in a 95% $O_2$/5% $CO_2$ environment at 36 °C. Thereafter, the KH solution was replaced by the experimental bath solution in which the bundles were very gently triturated to yield single fibres. The experimental bath solution was pre-gassed with $O_2$ and contained (in mM): NaCl 145, KCl 5, $CaCl_2$ 0.5, $MgCl_2$ 1, glucose 5 and MOPS 10. About 5 ml/l 1 M NaOH was used to adjust the pH to 7.2, making the final sodium concentration 150 mM and osmolality approximately 300 mOsm. Directly after trituration, the fibres were stored in an $O_2$ environment or placed in the measuring chamber (Leiden chamber; [17]) with $O_2$ superfusion at room temperature. Only fibres that displayed clearly visible cross-striations were used for the experiments. Preliminarily, we found that these fibres were capable of contracting. Visible $K^+$-elicited contractions could be obtained when positive pressure was applied to electrodes with wide tips containing a high $[K^+]$.

Borosilicate electrodes with filament (Hilgenberg, Malsfeld, Germany) were pulled on a microelectrode puller (P-97, Sutter Instruments, Novato, Calif., USA) and backfilled (3–7 MΩ) with the following solution (mM): KCl 150, $CaCl_2$ 2, MOPS 10 and 9-AC 0.075. 9-AC was added to the patch solution to prevent interference by the homogeneous $Cl^-$ conductance in the skeletal muscle [28]. About 5 ml/l 1 M KOH was used to adjust the pH to 7.2, making the final $[K^+]$ 155 mM. The pipette solution was degassed for noise reduction and had an osmolality of approximately 305 mOsm.

After establishing a seal (2–5 GΩ), recordings were performed in the cell-attached patch configuration [14] at room temperature (~22 °C). Single-channel currents were recorded using an Axopatch 200A amplifier (Axon Instruments, Union City, Calif., USA). The recording filter bandwidth was 2 kHz for amplitudes lower than 4 pA and 10 kHz for larger amplitudes. Recordings were controlled by pClamp7 software and digitized (20 kHz) through a Digidata 1200 series interface (Axon Instruments). After seal formation, a command potential ($V_c$), which is expressed inside the cell relative to outside, was applied.

In a typical protocol, the channel in the patch was characterized by its current response to a series of randomly chosen voltages ($-120\ mV<V_c<100\ mV$; in steps of 10 mV). After this characterization and identification the bath solution was changed by gentle injection of 3 ml bath solution containing 1 μM Iso into the measuring chamber. After about 2 min, the same volume was withdrawn from the chamber using gentle suction. Solution changes were carried out carefully and slowly (~5 min), in order to maintain background noise levels comparably low and because test experiments (without Iso) showed that perfusion should be slow to prevent fibre contractions. The estimated final [Iso] was 0.5 μM. About 7 min after the first series, a new $V_c$ series was applied, now in the presence of Iso. The total protocol took approximately 20 min to execute. The choice of Iso concentration and wash-in times was based on previous experiments [37]. In those experiments the [Iso] eliciting a half-maximal response was 20 nM, the time taken for Iso to achieve its maximal effect was 5 min (for wash-in time course see also Fig. 5) and the time, after complete Iso removal, for the cell to return to baseline was 45 min [37]. In addition, only one supramaximal Iso concentration was used, because these long wash-out times prevented construction of reliable concentration/response curves in one cell. Moreover there is no straight-forward method for extrapolating single-channel data at different concentrations to cellular behaviour. Stable seals could rarely be maintained for longer than 30 min. Therefore, Iso wash-out patch experiments were not possible. Sometimes circumstances required deviations from the typical protocol: either Iso could not be applied before seal breakdown or Iso was already applied before control.

For data analysis of the patch-clamp records, the QuB program suite (Department of Physiology and Biophysics, State University of New York at Buffalo) was used (www.qub.buffalo.edu). Data were pre-processed with QuB, where baseline was corrected and sampling was adjusted to twice the bandwidth. Slope conductances of the $i/V$ relationship ($\gamma$) and the reversal potential ($V_{rev}$) at the voltage intersection were determined by fitting unitary amplitudes in a $i/V$ diagram with a linear function (e.g. Fig. 1B). Only inwards slope conductances were used, because inwards currents behaved linearly, whereas outward currents often did not.

The dependence of the steady-state probability of the channel being open ($P_{open}$) on $V_c$ was fitted to the Boltzmann equation:

$$P_{open}(V_c) = \frac{P_{open,max}}{1 + \exp\left(\frac{V_c - V_{1/2}}{k}\right)}$$

where $P_{open,max}$ represents the maximum $P_{open}$, $V_{1/2}$ the voltage at which $P_{open}(V_c)$ is half-maximal and $k$ the term for the voltage dependence of activation.

Two operational criteria were used to identify and characterize $K^+$ channels. The first was whether strong inwards rectification was apparent near $V_{rev}$, and the second was whether $\gamma$ exceeded 100 pS. In the case where the first criterion was met, the channel was identified as an $K_{IR}$ channel (see Fig. 1B). Once an $K_{IR}$ channel was found, $V_{rev}$ was identified as the Nernst (equilibrium) potential for $K^+$ ($E_K$), since it is well known that the potential at which the $K_{IR}$ channel stops conducting is $E_K$ [16, 18, 19, 22, 23, 26, 31]. On the other hand, when $\gamma$ exceeded 100 pS and no clear rectification was found at $V_{rev}$, the channel was identified as a BK channel (see Fig. 2B). The two operational criteria were never met simultaneously in one patch.

### Intracellular microelectrodes

All materials and methods for these measurements were as described previously [13]. Briefly, KH solution was used and the $[K^+]_o$ was varied by equimolar replacement of KCl by NaCl or vice versa. Polyethyleneglycol 400 was added to increase osmolality from 290 to 344 mOsm. Iso (0.2–1 μM), bumetanide (75 μM) and 9-AC (75 μM) were added in supra-maximal concentrations. In the chamber the solution temperature was adjusted to 35 °C. Fine-tipped glass microelectrodes (filled with 3 M KCl; tip resistance 25–80 MΩ) were used to measure $V_m$. The output of the microelectrode amplifier (M4-A, WPI, Sarasota, Fla., USA) and the output of the reference microelectrode in the bath were sampled at 1 kHz. The data over 1 s were averaged and stored using LabView 3.1 (National Instruments, Austin Tex., USA). The difference between the outputs was the cell membrane potential (negative inside).

Staircase protocols were used to record hysteresis of $V_m$ (as illustrated in Fig. 4, open and closed squares). $[K^+]_o$ was reduced in small (10%) steps by replacing it with $Na^+$. Following one of the reduction steps in $[K^+]_o$ a massive depolarization was observed: this concentration was called the "switch-off" concentration (Fig. 4,

closed squares at $[K^+]_o$=1.6 mM). Thereafter, $[K^+]_o$ was increased stepwise and after an increasing step a large hyperpolarization occurred: this concentration was called the "switch-on" concentration (Fig. 4, open squares at $[K^+]_o$=2.02 mM). Hysteresis was present when the switch-off concentration was smaller than the switch-on (see squares in Fig. 4). The terms switch-off and switch-on refer to the behaviour of the $K_{IR}$, which closed (i.e. switched off) or opened (i.e. switched on) at these $[K^+]_o$ [13]. The cell was allowed to equilibrate for 4 min at each concentration and for 45 min when a switch had occurred. After a control protocol in isotonic media had been completed, a second staircase protocol in the presence of Iso was attempted (Fig. 4). The completion of two successive full staircase protocols in one cell took about 3 h; during which neither the impalement should have been compromised nor the cell have deteriorated.

### Statistics

Steady-state data are presented as means±SEM with the number of observations ($n$) in parentheses. The significance of differences between means was assessed with Student's $t$-test ($n \geq 5$). The correlation coefficient ($r$) is given when a curve was fitted to data.

### Chemicals

All chemicals were analytical grade; salts were obtained from Janssen Chimica (Geel, Belgium), and all other chemicals from Sigma.

## Results

### Cell attached patches

#### *$K^+$ channel identification and characterization*

A total of 119 seals were formed, of which 38 displayed single-channel activity and about 20 contained multiple channels. The latter were excluded from further analysis. In 24 patches the channels could be identified using the operational criteria for identification and characterization. A total of 14 patches did not meet either criterion and were not studied further.

#### *Characterization of strongly inwardly rectifying channels*

Some 13 channels were identified as $K_{IR}$ by virtue of the strong inwards rectification properties. The channels ceased to conduct detectably at potentials positive to $V_{rev}$ (mean 21 mV; Table 1). The inwards conductance was 45±3 pS (Table 1 and Fig. 1B, see also [18]). The current records (Fig. 1A) displayed long-lasting stable open intervals typical for $K_{IR}$ channels [19, 23, 26]. Sometimes sublevel currents at approximately 80% of maximum value were found [26]. $P_{open}$ of the $K_{IR}$ channel increased with depolarization (Fig. 1C). The corresponding $V_{1/2}$ was −27 mV (Table 1). These *i/V* characteristics, open-closed behaviour and the voltage dependence of $P_{open}$ are hallmarks for the $K_{IR}$ channel [5, 19, 21, 22, 23, 24, 26, 31].

In seven patches in which $K_{IR}$ channels were identified in the absence of Iso, no $K_{IR}$ channel activity could be distinguished from background noise after application of Iso at $V_c$ between −100 and 100 mV (Table 1 and Fig. 1D). However, the noise in the closed state increased significantly from 0.61 to 1.4 pA ($P$<0.01).

#### *Characterization of channels with a conductance larger than 100 pS (BK)*

A second type of channel was recorded in eight cells. It displayed fast transitions (Fig. 2A), had a high inwards slope conductance (181 pS; Table 1) and a $V_{rev}$ at 22.6 mV (Table 1). This $V_{rev}$ did not differ significantly from that of the $K_{IR}$ ($P$>0.05), as might be expected for a $K^+$ channel. The *i/V* relation of this channel showed some inwards rectification (Fig. 2B and D), but much less than $K_{IR}$, and rectification occurred at potentials positive to $V_{rev}$. $P_{open}$ was also voltage dependent, but was small for most $V_c$ (Fig. 2E open symbols). $V_{1/2}$ was 50 mV (Table 1), which was considerably more positive than $V_{rev}$. Even though this channel opened sporadically at very negative potentials, these openings were sufficient to detect its presence. In summary, this channel exhibited the following properties: (1) a unitary channel conductance (155 mM $K^+$ in the patch pipette) of 181 pS, (2)

**Table 1** Influence of isoprenaline on the characteristics of single, inwardly rectifying ($K_{IR}$) and $Ca^{2+}$-activated, large-conductance ($BK$) $K^+$ channels in skeletal muscle plasma membrane. $n$ is the number of patches, $n_p$ is the number of patches for which paired control and isoprenaline results were obtained and *values* in *parentheses* indicate the number of determinations when they differ from $n$. This was the case when the points were not spaced well or too few points were recorded to fit data to the Boltzmann equation (see text for symbols). Root-mean-square noise was determined in closed state at 2 kHz bandwidth

| Channel type | $n$ | $n_p$ | $\gamma$ (pS) | $P_{open,max}$ | $V_{1/2}$ (mV) | $V_{rev}$ (mV) | $k$ (mV) | Closed noise (pA) |
|---|---|---|---|---|---|---|---|---|
| Control | | | | | | | | |
| $K_{IR}$ | 13 | 7 | 45±3 | 0.93±0.01 (8) | −27±14 (8) | 21.0±4.8 | −15±2.6 (8) | 0.61±0.08 |
| BK | 8 | 3 | 181±15§ | 0.84±0.01 (5) | 50±3.0§ (5) | 22.6±5.5 | −11±0.3 (5) | 0.83±0.15 |
| Isoprenaline | | | | | | | | |
| $K_{IR}$ | 7 | | | | | | | 1.4±0.4* |
| BK | 6 | | 160±8 | 0.90±0.04 (5) | −40±3.7* (5) | 25.2±2.4 | −14±1.5 (5) | 0.70±0.10 |

§$P$<0.01 vs. $K_{IR}$ in control
*$P$<0.01 for Iso vs. control for the same channel

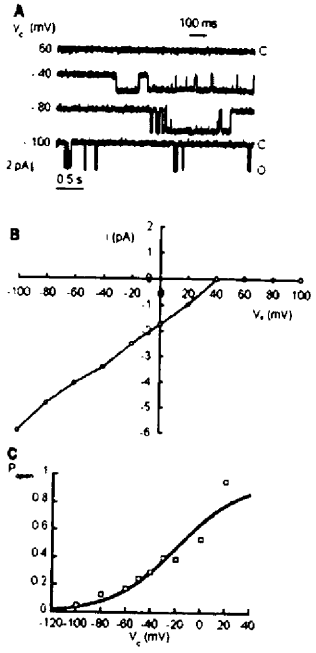


**Fig. 1A–C** A typical example of the characteristics of a single inwardly rectifying $K^+$ ($K_{IR}$) channel. **A** Unitary $K_{IR}$ channel currents in cell-attached patches at different command potentials ($V_c$). *Downwards* current deflections are openings (*O*). The *top three traces* are stretches of 1250 ms, for which the 100-ms *scale bar* applies. The *bottom trace* (−100 mV), for which the 0.5-s *scale bar* applies, is resampled to fit a stretch of 15 s to demonstrate the long closed times. Filtering is set at 2 kHz. **B** Current/voltage (*i/V*) relation of the $K_{IR}$ channel. The inwards slope conductance was 40.4 pS. **C** Open probability ($P_{open}$) as function of $V_c$. Fitting the data to the Boltzmann equation (see text for abbreviations) yielded $P_{open,max}$=0.95, $V_{1/2}$=−18 mV and $k$=−26 mV, $r$=0.97

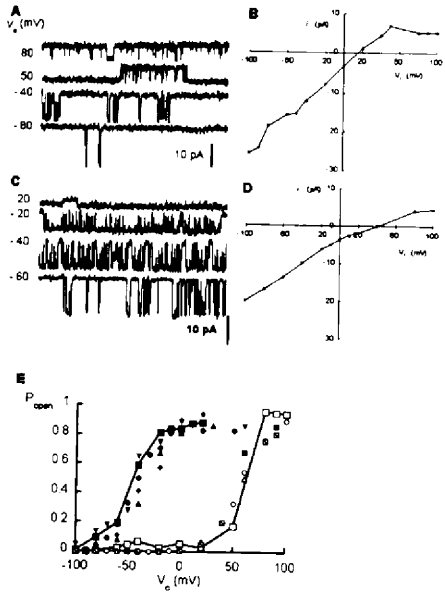


**Fig. 2A–E** A typical example of the characteristics of a single large-conductance, $Ca^{2+}$-activated $K^+$ (BK) channel in the presence and absence of isoprenaline (Iso). **A** Unitary BK channel currents in the cell-attached configuration at various $V_c$. The *upwards* current *deflections* at $V_c$=50 and 80 mV and the *downwards* current *deflections* at $V_c$=−40 and −80 mV are openings. The stretches are 250 ms long and filtering is set at 2 kHz for display. Note the very long closure times in the *bottom three traces*. **B** *i/V* relation of BK. Linear extrapolation (see Materials and Methods) of the inward currents gives: $i$=0.219$V_c$−3.3 ($i$ in pA, $V_c$ in mV); $r$=0.99. The inwards slope conductance was 219 pS, the reversal potential ($V_{rev}$) 15.1 mV. **C** Unitary currents from the same BK channel as in **A** at various $V_c$ after application of Iso. *Downwards deflections* are openings. Interval length and filtering as in **A**. Occasional sublevel deflections were recorded (approximately 60% of maximum amplitude), as apparent at $V_c$=−40 mV. **D** *i/V* relationship of the BK channel after application of Iso. Linear extrapolation of the inward currents gives: $i$=0.158$V_c$−4.0; $r$=0.99. Inwards slope conductance was 158 pS and $V_{rev}$ 25.3 mV. **E** $P_{open}/V_c$ relationship for BK channels ($n$=7). *Open symbols*: $P_{open}$ in the absence of Iso, *filled symbols*: $P_{open}$ in the presence of Iso. *Similar symbols* (*squares*, *circles* and *upright triangles*) are from three patches in which Iso and non-Iso records are paired. The *connected squares*, *open* and *filled*, are from the same patch as **A**–**D**. The mean values obtained from the Boltzmann equation are given in Table 1

zero current at $V_c$=$E_K$ according to the interpretation given for $K_{IR}$ and (3) a decrease of $P_{open}$ as $V_c$ became more negative. These properties identified this channel as belonging to the skeletal muscle BK-channel family [2, 25, 29, 36].

In three patches the activity of a BK channel after application of Iso was compared with the activity directly before Iso. Three other fibres were patched during exposure to Iso. Results of the measurements in these fibres corroborated the results of paired measurements when Iso was present. This applied to the measured $V_{rev}$, $\gamma$ or closed channel noise ($P$>0.05, Table 1). The main influence of Iso was an approximately 90 mV negative shift in $V_{1/2}$ (Fig. 2E open vs. filled symbols) from 50 mV before application of Iso to −40 mV ($P$<0.01) after (Table 1). $V_{1/2}$ was 65 mV negative with respect to $V_{rev}$ and Fig. 2E (filled symbols) confirmed that BK channels were very active at physiological potentials in the presence of Iso. Noise did not increase (Table 1).

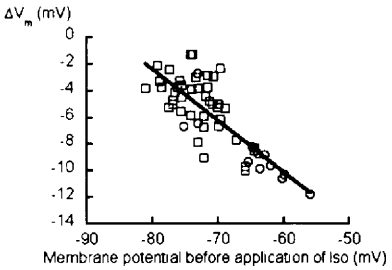


**Fig. 3** Voltage dependence of the hyperpolarization elicited by Iso in isotonic (*open squares*) and hypertonic (*open circles*) media with $[K^+]_o$=5.7 mM. The Iso-induced hyperpolarization is displayed as a function of the membrane potential ($V_m$) prior to its addition. The linear regression was $\Delta V_m$=−33.3−0.387$V_{m,pre}$, $r$=0.80

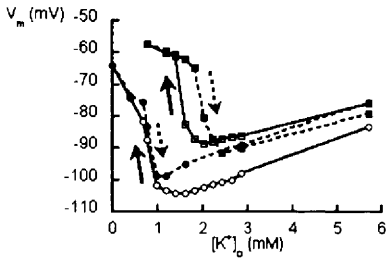


**Fig. 4** Isoprenaline abolished the hysteresis of $V_m$ due to the change in $[K^+]_o$. $[K^+]_o$ was first reduced from 5.7 to 0.76 mM (the *solid line* through the *open squares*). The "switch-off" $[K^+]_o$ (see text) was 1.6 mM. Then $[K^+]_o$ was increased, returning to 5.7 mM, for which the "switch-on" $[K^+]_o$ was 2.02 mM (the *dashed line* through the *filled squares*). After addition of Iso, the staircase was repeated, whereby $[K^+]_o$ was reduced from 5.7 to 0 mM (the *solid line* through the *open circles*) and back again (the *dashed line* through the *filled circles*). Note that the large change in $V_m$ occurs below 1 mM, that several steady $V_m$ values are recorded during this $\Delta V_m$ and that no hysteresis was found during this staircase. When $[K^+]_o$>1 mM the $V_m$ values in this return trajectory do not coincide fully with the corresponding values in the descending trajectory. We attributed this to the fact that the cell was exposed for ~15 min to nominally $[K^+]_o$=0 mM

## Intracellular microelectrode results

### *Isoprenaline-induced hyperpolarization as function of $V_m$*

In isotonic ($n$=42) and hypertonic ($n$=12) media with $[K^+]_o$=5.7 mM the maximal hyperpolarization ($\Delta V_m$) induced by Iso was 12 mV (Fig. 3). The mean responses to Iso in isotonic and hypertonic media were −4.9±0.3 and −8.6±0.7 mV respectively ($P$<0.01). A correlation existed between $V_m$ prior to Iso ($V_{m,pre}$) and the $\Delta V_m$ (linear regression: $\Delta V_m$=−33.3−0.387$V_{m,pre}$).

### *The disappearance of the hysteresis loop due to isoprenaline*

The cell-attached experiments showed that besides $K_{IR}$, other $K^+$ channels with different $i/V$ behaviour and responsiveness to Iso are present in the resting muscle. This prompted us to determine the hysteresis of $V_m$ in the presence and absence of Iso (Fig. 4). In control media, a hysteresis loop with two large discontinuous potential changes ($|\Delta V_m|$>25 mV) was observed (Fig. 4, squares). The switch-off $[K^+]_o$ (see Materials and methods) was 1.6 mM and the switch-on 2.02 mM. In contrast, in the presence of Iso (Fig. 4, circles) the cell responded differently to the staircase protocol. The hysteresis disappeared and the depolarization occurred at lower $[K^+]_o$ (<1 mM) as a continuous process (between ~−100 and −65 mV). Therefore, switch-on and switch-off concentrations could not be defined in the presence of Iso. These results were confirmed in the two other fibres in which the double staircase protocols were performed.

### *Influences that vary the magnitude of the Iso hyperpolarization*

To obtain more insight into how the Iso response depended on other parameters, experiments were carried out under a variety of different conditions.

*Low extracellular K+.* On inspection of the hysteresis loop in control media (Fig. 4), it seemed obvious that two stable membrane potentials could be found in some media with lowered $[K^+]_o$. However, when fibres were preincubated with Iso this bistable behaviour disappeared. In comparison to Fig. 4, the Iso response at $[K^+]_o$=0.76 mM was always more negative than −10 mV irrespective of whether cells were depolarized or hyperpolarized ($P$<0.01; Table 2). Typical examples of Iso responses at $[K^+]_o$=0.76 mM in depolarized (Fig. 5A) and hyperpolarized (Fig. 5B) fibres were compared with the Iso-induced hyperpolarization at $[K^+]_o$=5.7 mM in one and the same cell.

*Chloride transport.* The magnitude of the Iso-induced hyperpolarization was dependent on the $V_{m,pre}$ both in iso- and hypertonic conditions (Fig. 3). Previously, it has been reported that hypertonic solutions induce a depolarization of the cell (upper trace in Fig. 6) and that this depolarization is prevented when bumetanide is given prior to the hypertonic shock (second trace in Fig. 6) [38]. In addition, preincubation with Iso inhibited the depolarization caused by hypertonic solutions (third trace of Fig. 6; $\Delta V_m$=2.5±1 mV, $n$=9). This was not different from

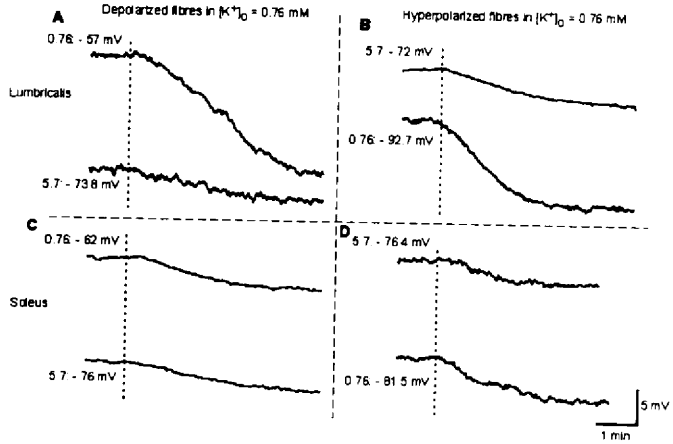


**Fig. 5A–D** Four examples in which Iso was applied at $[K^+]_o$=5.7 and 0.76 mM to one and same fibre. The *dotted lines* indicate the point of Iso application, the *bars* in the *bottom right-hand corner* are the time and voltage scales. $[K^+]_o$ and the starting voltages are given *beside* the trace. **A** Iso applied to a lumbrical fibre at $[K^+]_o$=5.7 and 0.76 mM. This fibre depolarized in the presence of $[K^+]_o$=0.76 mM. This protocol was repeated in seven other fibres, where the Iso response in $[K^+]_o$=0.76 mM was significantly larger than in $[K^+]_o$=5.7 mM ($P$<0.01). **B** Iso applied to a lumbrical fibre in $[K^+]_o$=5.7 and 0.76 mM. This fibre hyperpolarized in the presence of $[K^+]_o$=0.76 mM. Six experiments of this protocol were carried out in the extensor digitorum longus muscle, the results were similar to that in the lumbrical muscle. **C** Iso applied to a soleus fibre in $[K^+]_o$=5.7 and 0.76 mM. This fibre depolarized in the presence of $[K^+]_o$=0.76 mM. **D** Iso applied to a soleus fibre in $[K^+]_o$=5.7 and 0.76 mM. This fibre hyperpolarized in the presence of $[K^+]_o$=0.76 mM. Interestingly, all recordings display a sigmoid behaviour. This implicates, that multiple processes underlie the Iso-induced hyperpolarization

**Table 2** Negative potential shifts induced by isoprenaline at $[K^+]_o$=0.76 mM in cells that were either depolarized or hyperpolarized with respect to control media. Isoprenaline was applied to cells with stable membrane potentials ($V_m$) in $[K^+]_o$=0.76 mM that are either depolarized or hyperpolarized compared with $[K^+]_o$=5.7 mM. $V_{m,pre}$ is $V_m$ directly before application of Iso, $\Delta V_m$ the change in $V_m$ induced by Iso. The $P$ values refer to the comparison between Iso application in different conditions and Iso application in the depolarized state in the same muscle (*NS* not significant)

| Muscle | | $V_{m,pre}$ (mV) | $\Delta V_m$ (mV) | $n$ | $P$ |
|---|---|---|---|---|---|
| Lumbricalis | depolarized | −51.9±0.6 | −11.4±0.5 | 73 | |
| | hyperpolarized | −94.8±2.8 | −15.8±1.9 | 5 | <0.05 |
| Soleus | depolarized | −60.5±2.9 | −4.7±0.8* | 5 | |
| | hyperpolarized | −94.3±3.5 | −6.2±1.3* | 6 | NS |

*$P$<0.01 for soleus vs. lumbricalis

the preincubation with bumetanide ($\Delta V_m$=0.6±0.5 mV, $n$=15, and with 3-isobutyl-1-methylxanthine (IBMX) (200 μM; bottom trace in Fig. 6; $\Delta V_m$=2.4±0.8 mV $n$=4). However, this effect was not purely competitive, because bumetanide caused significant membrane hyperpolarization in the presence of Iso (1.4±0.8 mV $n$=7; $P$<0.05 in paired experiments).

*Muscle type.* For comparison with lumbrical muscle, data obtained under identical conditions in soleus muscle are shown in the bottom two rows of Table 2. The fibres of the soleus also exhibited bistable behaviour at $[K^+]_o$=0.76 mM: some cells depolarized, whereas others hyperpolarized [12, 13, 27]. Both the depolarized and the hyperpolarized soleus fibres became more negative when Iso was added, but the change was significantly smaller than in lumbrical fibres (Table 2). Additionally, in the soleus, the negative potential change due to Iso application in media with $[K^+]_o$=0.76 mM did not differ significantly in paired experiments in control media ($n$=5) (Fig. 5C and D).

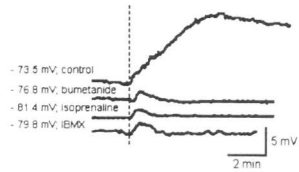


**Fig. 6** Isoprenaline and bumetanide prevent the depolarization induced by hypertonicity similarly. The *dashed line* indicates the time at which the medium osmolality was increased from 289 to 344 mOsm. The *top three traces* originate from the same cell, the *bottom trace* from a separate cell. The control response to the switch in osmolality (*upper trace*) was a depolarization of about 10 mV. This depolarization was prevented by preincubation with 75 μM bumetanide (*second trace* from the *top*), 1 μM Iso (*third trace*) or 200 μM 3-isobutyl-1-methylxanthine (IBMX, *lowest trace*). $V_m$ before the solution switch is given at the *left* of the trace, as is the preincubated substance. The transient immediately following the hypertonic shock was not a switching artefact. The time courses of the transient responses to hypertonicity after bumetanide, Iso and IBMX preincubations were similar. The *bars* in the *lower right-hand corner* are the time and $V_m$ scales

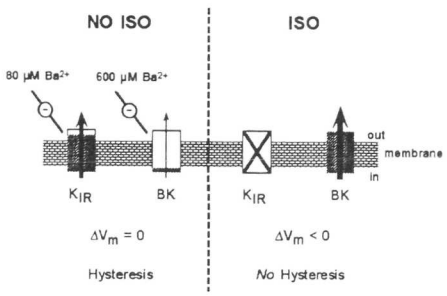


**Fig. 7** A schematic representation of the $K^+$ conductive pathways underlying the Iso-induced hyperpolarization. This scheme summarizes the present data and earlier [37] data. The *arrows* display the direction of $K^+$ current through the channels, whereby the width of the arrows indicates approximately the relative amount of current flowing through the individual channel. *Left*: a control (no Iso) skeletal muscle membrane is shown with two $K^+$ channels, $K_{IR}$ and BK. $K_{IR}$ conducts considerably more current in these conditions than BK. Under these conditions the cell can exhibit hysteresis of $V_m$. Both channels can be inhibited by extracellular $Ba^{2+}$: $K_{IR}$ at 80 and BK at 600 μM. *Right*: an Iso-stimulated skeletal muscle membrane is illustrated. $K_{IR}$ is now (nearly) closed and BK dominates. Hyperpolarization results when the sum of $K^+$ currents increases in comparison to control cells. Under these conditions, due to the properties of BK channels, the cell does not exhibit hysteresis of $V_m$

## Discussion

The combined approach of cell-attached and intracellular microelectrode measurements provides information about the behaviour of $K^+$ channels and their consequences for the cell's membrane potential (Fig. 7). Firstly, the cell-attached experiments infer the functional presence of $K_{IR}$ and BK channels in the sarcolemma of skeletal muscle, where $K_{IR}$ dominates $P_K$ under control conditions. Channel characterization is consistent with reports in literature for $K_{IR}$ [5, 19, 21, 22, 23, 24, 26, 31] and BK [2, 25, 29, 36] channels. Additionally, due to the circumstance that the activity of $K_{IR}$ decreases and that of BK increases following application of Iso under identical experimental conditions, it is concluded that the effect of the increased BK contribution induced by Iso exceeds the concomitant effect of the decrease of the $K_{IR}$. Secondly, the intracellular microelectrode experiments show a loss of hysteresis of $V_m$, indicating a loss of $K_{IR}$ activity after application of Iso. The results suggest that the activation of BK channels is mediated by $Ca^{2+}_i$, but also that other experimental conditions influence the responses (e.g. $V_{m,pre}$, $[K^+]_o$, chloride transport and muscle type). Finally, the combination of experimental techniques uncovered the differential cellular conductive response in hypokalaemic conditions in control and $\beta_2$-adrenergically stimulated fibres.

### The influence of isoprenaline on $K^+$ channels

$\beta_2$-Adrenergic modulation of $K^+$ channel activity has, to our knowledge, not yet been studied in skeletal muscle. The application of Iso causes the $K_{IR}$ and BK channel to respond differently. Firstly, the single channel activity of the $K_{IR}$ is suppressed at $V_c$ values in the range of normal resting membrane potential. Similarly, Iso application suppresses cell-attached $K_{IR}$ activity after a direct phosphorylation event in guinea-pig ventricle [19]. In addition to the decreased $K_{IR}$ activity, current noise increases two-fold, which is not observed in patches with BK channels. This increased noise might be an indication of a very short-lived low (sub)-conductance state of the $K_{IR}$ channel. Low conductance levels for the $K_{IR}$ channel have been demonstrated [7].

Secondly, the activity of BK channels increased, which is expressed as a 90-mV negative shift of $V_{1/2}$ (Fig. 2E), without a change in single-channel conductance. This shift of $V_{1/2}$ is 10 times more than the change of the resting membrane potential itself, which is maximally −12 mV (Fig. 3). Because $V_{rev}$ for BK with or without Iso are not significantly different (Table 1), a large change in $E_K$ is unlikely. The temperature difference between the cell-attached and intracellular microelectrode experiments does not seem to have contributed considerably to the 90 mV negative shift in $V_{1/2}$, because in mouse diaphragm at room temperature a hyperpolarization of the cell is recorded after application of Iso [41]. Therefore, the increased activity is probably a change in the properties of the BK channel itself.

### Cellular responses to isoprenaline

Iso causes a loss of hysteresis and discontinuity of $V_m$ as a function of $[K^+]_o$ (Fig. 4). Hysteresis is found when the contribution of the $K_{IR}$ dominates in $P_K$ [12, 13] of unclamped cells, because its open-close kinetics depends on the $K^+$ gradient across the membrane [33, 34]. These kinetic properties explain equally well the hysteresis loop we measured as well as the N-shaped $i/V$ curve observed by others [4, 10, 40] during voltage-clamp experiments of cells with $K_{IR}$ in their membranes [34]. This dependence introduces a threshold that makes the channels open and close in a regenerative way. This is not the case with the BK channels, which do not possess such kinetics [8]. Thus, when the permeability of the BK channels dominates $P_K$, hysteresis will not be expected (Fig. 4). This is in accordance with our findings. The negative correlation found between $V_{m,pre}$ and the hyperpolarization induced by Iso (Fig. 3) can be related to the voltage-dependent activation of the BK channels. The route of regulation of these channels by Iso is mediated by the $\beta_2$-adrenoceptor and subsequently via a cAMP-activated pathway [37]. Also $[Ca^{2+}]_i$ seems to be implicated as in mouse diaphragm muscle a suppression of the hyperpolarizing response to $\beta$-mimetica is found after calcium is left out of the medium for 30 min [41].

Bumetanide can prevent the depolarization induced by hypertonic stress [38] and Iso or IBMX have the same effect. Perhaps the same cellular processes for instance the cAMP pathway, that induced the closure of the $K_{IR}$ also prevent the cotransporter from having the same effects on $V_m$ as in isotonic conditions.

The hyperpolarization induced by Iso can be explained when the loss of one $K^+$ conductance ($K_{IR}$) is overcompensated by another $K^+$ conductance (BK). Sufficient BK channels are required in the membrane. This is in line with the statistics of Table 1. In the soleus muscle $\beta_2$-adrenergic stimulation reportedly increases Na/K-pump activity [6]. However, in lumbrical muscle Iso still makes $V_m$ more negative when the Na/K-pump is inhibited with ouabain [37]. In a direct comparison of both muscles, we found that in soleus the hyperpolarization induced by Iso is smaller and apparently not $[K^+]_o$ dependent (Table 2). Such differences can easily be explained when the ratio of BK conductance to $K_{IR}$ conductance is variable. These findings might be an experimental indication that functional differences in muscle fibre types are also related to the differential expression of ion channels in their membranes. This may be of importance for the differential response of the muscles to adrenaline in the whole body. The catecholamine concentrations in the body will normally be less than the supramaximal concentration used here. However, variations of catecholamine concentrations will modulate the ratio of BK conductance over $K_{IR}$ conductance in the same direction as presented here.

### Hypokalaemic periodic paralysis

Hypokalaemic periodic paralysis is accompanied by a decrease in serum $[K^+]$ and a simultaneous depolarization of the fibre. A loss of function of $K_{IR}$ in relation to hypokalaemic periodic paralysis has been reported several times. The cellular $K_{IR}$ conductance is decreased in fibres from patients suffering from hypokalaemic periodic paralysis [30]. Treatment with $Ba^{2+}$ [12], a known $K_{IR}$ blocker [35], and hysteresis of $V_m$ [12, 13] produce responses electrically similar to hypokalaemic periodic paralysis. Our results reveal differential responses of the important $K^+$ channels including the $Ca^{2+}$ sensitive BK channel. $\beta_2$-Adrenergic stimulation of these channels might provide a means for recovering the decreased $K^+$ conductance.

**Acknowledgements** We are grateful to the department of Physiology and Biophysics of the State University of New York at Buffalo, and to Lorin Milescu in particular, for the introduction to QuB. We are also grateful to Dr Gerard Borst for his advice and the use of the Sutter P-97 electrode puller, to Dr Wytse Wadman for his constructive remarks and to Dr Dirk Ypey for encouragement.

## References

1. Armstrong CM, Taylor SR (1980) Interaction of barium ions with potassium channels in squid giant axons. J Gen Physiol 30:473–488
2. Brinkmeier H, Zachar E, Rüdel R (1991) Voltage-dependent $K^+$ channels in the sarcolemma of mouse skeletal muscle. Pflugers Arch 419:486–491
3. Cairns SP, Dulhunty AF (1995) The effects of $\beta$-adrenoceptor activation on contraction in isolated fast- and slow-twitch skeletal muscle fibres of the rat. Br J Pharmacol 110:1166–1141
4. Carmeliet E (1982) Induction, removal of inward-going rectification in sheep cardiac Purkinje fibres. J Physiol (Lond) 327:285–308
5. Choe H, Sackin H, Palmer LG (2001) Gating properties of inward-rectifier potassium channels: effects of permeant ions. J Membr Biol 184:81–89
6. Clausen T, Overgaard K (2000) The role of $K^+$ channels in the force recovery elicited by $Na^+$-$K^+$ pump stimulation in $Ba^{2+}$-paralysed rat skeletal muscle. J Physiol (Lond) 527:325–332
7. Cohen IS, DiFrancesco D, Mulrine NK, Pennefather P (1989) Internal and external $K^+$ help gate the inward rectifier. Biophys J 55:197–202
8. Conley EC (1996) Intracellular calcium-activated $K^+$ channels (KCa). In: Conley EC (ed) The ion channel facts book II. Intracellular ligand-gated channels. Academic Press, New York, Entry 27
9. Flatman PW, Creanor J (1999) Regulation of $Na^+$-$K^+$-$2Cl^-$ cotransport by protein phosphorylation in ferret erythrocytes. J Physiol (Lond) 517: 699–708
10. Gadsby DC, Cranefield PF (1977) Two levels of resting potential in cardiac Purkinje fibers. J Gen Physiol 70:725–746
11. Gallant EM (1983) Barium-treated mammalian skeletal muscle: similarities to hypokalaemic periodic paralysis. J Physiol (Lond) 335:577–590
12. Geukes Foppen RJ, Van Mil HGJ, Siegenbeek van Heukelom J (2001) Osmolality influences bistability of membrane potential under hypokalaemic conditions in mouse skeletal muscle: an experimental and theoretical study. Comp Biochem Physiol [A] 130:533–538

13. Geukes Foppen RJ, Van Mil HGJ, Siegenbeek van Heukelom J (2002) Effects of chloride transport on bistable behaviour of the membrane potential in mouse skeletal muscle. J Physiol (Lond) 542:181–191
14. Hamill OP, Marty A, Neher E, Sakmann B, Sigworth FJ (1981) Improved patch-clamp techniques for high-resolution current recording from cells and cell-free membrane patches. Pflugers Arch 391:85–100
15. Harvey RD, Hume JR (1989) Isoproterenol activates a chloride current, not the transient outward current, in rabbit ventricular myocytes. Am J Physiol 257:C1177–C1181
16. Hille B (1992) Ionic channels of excitable membranes, 2nd Edn. Sinauer, Sunderland
17. Ince C, Beekman RE, Verschragen G (1990) A micro-perfusion chamber for single-cell fluorescence measurements. J Immunol Methods 128:227–234
18. Kell MJ, DeFelice LJ (1988) Surface charge near the cardiac inward-rectifier channel measured from single-channel conductance. J Membr Biol 102:1–10
19. Koumi A, Wasserstrom JA, Ten Eick RE (1995) $\beta$-Adrenergic and cholinergic modulation of inward rectifier $K^+$ channel function and phosphorylation in guinea-pig ventricle. J Physiol (Lond) 486:661–678
20. Kuba K, Nohmi M (1987) Role of ion conductance changes and of the sodium-pump in adrenaline-induced hyperpolarization of rat diaphragm muscle fibres. Br J Pharmacol 91:671–681
21. Kubo Y, Baldwin TJ, Jan YN, Jan LY (1993) Primary structure and functional expression of a mouse inward rectifier potassium channel. Nature 362:127–133
22. Kurachi Y (1985) Voltage-dependent activation of the inward-rectifier potassium channel in the ventricular cell membrane of guinea-pig heart. J Physiol (Lond) 366:365–385
23. Kurtz R, Schirm T, Jockusch H (1999) Maturation and myotonia influence the abundance of cation channels $K_{DR}$, $K_{IR}$ and $C_{IR}$ differently: a patch-clamp study on mouse interosseus muscle fibres. Pflugers Arch 438:516–524
24. Lu T, Wu L, Xiao J, Yang J (2001) Permeant Ion-dependent changes in gating of Kir2.1 inward rectifier potassium channels. J Gen Physiol 118:509–521
25. Mallouk N, Jacquemond V, Allard B (2000) Elevated subsarcolemmal $Ca^{2+}$ in *mdx* mouse skeletal muscle fibers detected with $Ca^{2+}$-activated $K^+$ channels. Proc Natl Acad Sci USA 97:4950–4955
26. Matsuda H, Stanfield PR (1989) Single inwardly rectifying potassium channels in cultured muscle cells from rat and mouse. J Physiol (Lond) 414:111–124
27. Mølgaard H, Stürup-Johansen M, Flatman JA (1980) A dichotomy of the membrane potential response of rat soleus muscle fibres to low extracellular potassium concentrations. Pflugers Arch 383:181–184
28. Palade PT, Barchi RL (1977) On the inhibition of muscle chloride conductance by aromatic carboxylic acids. J Gen Physiol 69:879–896
29. Rothberg B, Magleby KL (1999) Gating kinetics of single large-conductance $Ca^{2+}$-activated $K^+$ channels in high $Ca^{2+}$ suggest a two-tiered allosteric gating mechanism. J Gen Physiol 114:93–124
30. Ruff RL (1999) Insulin acts in hypokalemic periodic paralysis by reducing inward rectifier $K^+$ current. Neurology 53:1556–1563
31. Sakmann B, Trube G (1984) Voltage-dependent inactivation of inward-rectifying single-channel currents in the guinea-pig heart cell membrane. J Physiol (Lond) 347:659–683
32. Sejersted OM, Sjøgaard G (2000) Dynamics and consequences of potassium shifts in skeletal muscle and heart during exercise. Physiol Rev 80:1411–1481
33. Siegenbeek van Heukelom J (1991) Role of the anomalous rectifier in determining membrane potentials of mouse muscle fibres at low extracellular $K^+$. J Physiol (Lond) 434:549–560
34. Siegenbeek van Heukelom J (1994) The role of the potassium inward rectifier in defining cell membrane potentials in low potassium media, analyzed by computer simulation. Biophys Chem 50:345–360
35. Standen NB, Stanfield PR (1978) Inward rectification in skeletal muscle: a blocking particle. Pflugers Arch 378:173–176
36. Tricarico D, Petruzzi R, Conte Camerino D (1997) Changes of the biophysical properties of calcium-activated potassium channels of rat skeletal muscle fibres during aging. Pflugers Arch 434:822–829
37. Van Mil HGJ, Kerkhof CJM, Siegenbeek van Heukelom J (1995) Modulation of the isoprenaline-induced membrane hyperpolarization of mouse skeletal muscle cells. Br J Pharmacol 116:2881–2888
38. Van Mil HGJ, Geukes Foppen RJ, Siegenbeek van Heukelom J (1997) The Influence of bumetanide on the membrane potential of mouse skeletal muscle cells in isotonic and hypertonic media. Br J Pharmacol 120:39–44
39. Vergara C, Latorre R (1983) Kinetics of $Ca^{2+}$-activated $K^+$ channels from rabbit muscle incorporated into planar bilayers. J Gen Physiol 82:543–568
40. Voets T, Droogmans G, Nilius B (1996) Membrane currents and the resting membrane potential in cultured bovine pulmonary artery endothelial cells. J Physiol (Lond) 49:95–107
41. Zemkova H, Svoboda P, Teisinger J, Vyskočyl F (1985) On the mechanism of catecholamine-induced hyperpolarization of skeletal muscle cells. Naunyn Schmiedeberg's Arch Pharmacol 329:18–23